Decision Analytics Journal 10 (2024) 100423

Contents lists available at ScienceDirect

Decision Analytics Journal

journal homepage: www.elsevier.com/locate/dajour

A simulation study to assess the epidemiological impact of pneumonia transmission dynamics in high-risk populations

C.W. Chukwu [a,*], S.Y. Tchoumi [b,c], M.L. Diagne [d]

[a] Department of Mathematics, Wake Forest University, Winston-Salem, NC 27109, USA
[b] Department of Mathematics and Computer Sciences ENSAI, University of NGaoundere, Cameroon
[c] Department of Mathematics and Applied Mathematics, University of Pretoria, South Africa
[d] Departement de Mathematiques, UFR des Sciences et Technologies, Universite de Thies, Thies, Senegal

ARTICLE INFO

Keywords:
Simulation
Dynamical system
Pneumonia
Sensitivity analysis
Treatment
High-risk population

ABSTRACT

The term "high-risk population" refers to individuals with an increased likelihood of contracting a severe illness or disease due to factors such as age, underlying medical conditions, pregnancy, geographical location, or a combination of these factors. This paper proposes a mathematical model of pneumonia focusing on the high-risk infected population: children under five years of age and adults over 65 years. A mathematical analysis is presented, and numerical simulations are conducted to investigate the impact of various model parameters on infection rates within each subpopulation. We employed Latin hypercube sampling for a global sensitivity analysis using the number of infectious individuals as a response function to identify the most influential parameters on the infection dynamics. Numerical results suggest that prompt and effective treatment at the onset of the disease is essential to control the spread of pneumonia among children under five and adults older than 65.

1. Introduction

Pneumonia is a contagious disease primarily caused by the bacterium Streptococcus pneumoniae (pneumococcus), whereas Mycoplasma pneumoniae is responsible for the infection in children [1]. It is a lung infection that can result in mild to severe illness in individuals across all age groups [2]. Pneumococcus spreads through the microaspiration of oropharyngeal organisms and the inhalation of aerosols containing bacteria or viruses. It may also spread via airborne droplets of cough or sneeze from an infected person. Notably, children can carry the bacteria in their throats without showing any symptoms of illness. Children can become severely ill with high fever and rapid breathing, while some may suffer convulsions, unconsciousness, hypothermia, lethargy, and feeding problems [3]. Limited data exists on the carriage of pneumonia infection among adult populations. Studies in [4,5] predicted that children remain the primary route of pneumonia spread to adults, especially in the household setting.

Recent statistics show that pneumonia is one of the most dangerous infectious diseases and causes high mortality rates in children worldwide [6]. Reports indicated that pneumonia was responsible for the death of about 740,180 children under five years old in 2019, accounting for 14% of the deaths of children under five years old [6]. Owing to the high mortality associated with pneumonia infection, the World Health Organization (WHO) and United Nations International Children's Emergency Fund have set the following goals to achieve by 2025: (i) reduce mortality from pneumonia in children less than 5 years of age to fewer than 3 per 1000 live births, (ii) to accelerate pneumonia control with a combination of interventions to protect, prevent, and treat pneumonia in children, that is, to protect children from pneumonia including promoting exclusive breastfeeding and adequate complementary feeding, (iii) prevent pneumonia with vaccinations, hand washing with soap, reducing household air pollution, and (iv) treat pneumonia by focusing on every sick child has access to the right kind of care, either from a community-based health worker or in a health facility [7].

The risk factors associated with the spread of pneumonia include smoking history (including passive smoking), malnutrition, crowded living conditions, indoor air pollution, heart disease, alcoholism, drug abuse, acidosis, diabetes, and antecedent viral infection, among other causes [8,9]. According to [1], pneumonia infections can be classified into the following categories: community-acquired, healthcare-associated, hospital-acquired, ventilator-associated, or walking Pneumonia, depending on its origin and the mode of transmission. After a person is infected with the disease and is diagnosed through an x-ray chest scan or blood tests, such as a complete blood count, appropriate antibiotics are used to treat bacterial pneumonia if that is the underlying cause of the pneumonia infection [3]. Effective and timely

* Corresponding author.
E-mail address: wiliam.chukwu@gmail.com (C.W. Chukwu).

https://doi.org/10.1016/j.dajour.2024.100423
Received 24 October 2023; Received in revised form 29 January 2024; Accepted 10 February 2024
Available online 13 February 2024

treatment, together with better diagnostic tools, can help prevent antibiotic resistance [10] in humans and thus decrease the tendency of relapse phenomena. According to Wardlaw et al. [11], treatment alone could save at least 600,000 children's lives annually at the cost of US $600 million if antibiotic treatment were universally delivered to children with pneumonia. Amoxicillin is recommended as a suitable alternative because of its proven efficacy against pneumococcus.

Several mathematical models have been developed to analyze the impact of pneumonia dynamics and possible means of disease eradication. We refer the interested reader to the following literature [12–17]. In particular, Idowu et al. [15] analyzed a Susceptible-Infected-Treatment mathematical model for the transmission dynamics of pneumonia among children under the age of 5. Their model suggested that increasing treatment and boosting children's immunity could lead to pneumonia eradication. Otieno et al. [17] presented a deterministic model for pneumonia dynamics with a carrier population for children under age 5 and found that reducing the transfer rates between the carrier and the infected class reduces the prevalence of the disease. In another study, Mary et al. [18] developed an optimal control model for managing the transmission dynamics of two strains of pneumonia. The study aimed to minimize the incidence of infections arising from drug-sensitive and drug-resistant strains, employing control measures such as educational campaigns, vaccination, and treatments. Kizito and Tumwiine [3] studied a Susceptible-Carrier-Infected-Vaccinated-Recovered compartmental model that incorporated treatment and vaccination interventions. The results from numerical simulations indicated that combining these interventions could lead to eradicating pneumonia. Furthermore, it found that with only treatment as an intervention, pneumonia infection will persist in the human population. Additional references on the dynamics of pneumonia in the context of control measures can be found in articles such as [19–26] among other published literatures.

Our present model stratifies the human population into the following classes: the elderly above 65, children under the age of 5, and adults between the ages of 5 and 64. Hence, our objective is to investigate the potential impact of the disease within these three sub-populations. This study aims to provide insights that can inform essential interventions needed to attain WHO 2025 goals and mitigate the infection dynamics of pneumonia among high-risk populations. In addition, our model will also study and predict several ways to lower infection dynamics by reducing high-risk factors causing the emergence/resurgence of pneumonia. To the best of our knowledge, no existing literature presents a model that explores the potential impact of pneumonia transmission pathways within the high-risk population using a deterministic approach. Therefore, we consider this work to be novel.

The road map for our work is as follows: In Section 2, we give the model formulation with the mathematical analysis presented in Section 3. The model is studied numerically, and the simulation results are given in Section 4. This paper is concluded in Section 5 with discussions as well as concluding remarks.

2. The model and its description

We formulate a sub-group population dynamics of pneumonia infection by considering a closed population consisting of three sub-groups of humans at high risk of infection. These three sub-groups are categorized into children under 5 years, individuals between the ages of 5 and 64, and adults above 65 years. Therefore, our model comprises 11 compartments described as follows: The Susceptible populations; over age 65 (S_a), between age 5 and 64 (S_m), and under age 5 (S_c), Exposed populations; over age 65 (E_a), between age 5 and 64 (E_m), under age 5 (E_c), Infectious populations; over age 65 (I_a), between age 5 and 64 (I_m), under age 5 (I_c), Treated population (T) and recovered population (R). Therefore, the total population at any time t is given as

Table 1
Description of model parameters, where resp. Means respectively.

Parameters	Biological interpretation	Units
β_i, for $i = 1, \dots, 3$	Contact rates for I_c, I_m, I_a resp.	day^{-1}
γ_h	Recovery rate	day^{-1}
$\alpha_c, \alpha_m, \alpha_a$	Treatment rates	day^{-1}
d_i, $i \in \{c, m, a\}$	Death rates for I_c, I_m, I_a resp.	day^{-1}
$\sigma_1(\sigma_2)$	Proportion of recovered who become $S_a(S_c)$	day^{-1}
μ_h	Natural mortality rate of human	day^{-1}
μ_i, $i \in \{c, m, a\}$	Natural death rates resp.	day^{-1}
η	Modification parameters for I_m	unitless
ξ	Rate of lost of immunity	day^{-1}
τ_i, for $i = 1, \dots, 3$	Progression rates for I_c, I_m, I_a resp.	day^{-1}
π_c	Recruitment rate of newborns into S_c	humans × day^{-1}
ϑ_{cm}	Maturation rate for S_c to S_m	day^{-1}
ϑ_{ma}	Maturation rate for S_m to S_a	day^{-1}

$$N(t) = S_c(t) + S_m(t) + S_a(t) + E_c(t) + E_m(t) + E_a(t) + I_c(t) + I_m(t) + I_a(t) + T(t) + R(t).$$

Let each subpopulation be assigned an indices i for ($i \in \{c, m, a\}$) representing children under 5 years (c), individuals between the ages of 5 and 64 (m), and adults above 65 years (a). Newborns are recruited only in the susceptible S_c with a constant recruitment rate π_c. These individuals after 5 years progress into the S_m at a maturation rate ϑ_{cm} and who in-turn move into the S_a class at a maturation rate defined as ϑ_{ma}. In contact with infectious individuals in the population, a susceptible individual can be exposed at a force of infection rates λ_i defined as

$$\lambda_c = \frac{\beta_c\left(I_c + \eta I_m + I_a\right)}{N}, \quad \lambda_m = \frac{\beta_m\left(I_c + \eta I_m + I_a\right)}{N}, \quad \lambda_a = \frac{\beta_a\left(I_c + \eta I_m + I_a\right)}{N}$$

and thus become infectious at a rate of τ_i. Here, the parameters β_i are the infection contact rates while η is the modification parameter for the I_m class only as they are assumed to be at low risk of contracting infectious comparable to I_c and I_a. Infectious individuals from I_i progress into T class at treatment rates α_i or die due to pneumonia at the rates of d_i. Once treated (those in T), they recover at rate γ_h and move into R class. The individuals in R may also lose their immunity after a certain time $\frac{1}{\xi}$, and become susceptible again by moving back into S_i classes with the probabilities σ_1, σ_2 and $(1-\sigma_1-\sigma_2)$ respectively. Susceptible, exposed, and infectious individuals in each sub-population may die naturally at a rate of μ_i respectively, and treated and recovered individuals in the population die at a constant rate of μ_h. Furthermore, we assume that all Pneumonia-infected individuals are treated at different rates α_i for each subpopulation respectively. The biological interpretation of the model parameters is explained in Table 1 while the model diagram is depicted in Fig. 1.

The deterministic system governing pneumonia transmission with the interaction between subpopulations and including our model assumptions yields:

$$\begin{cases} S_c' &= \pi_c + \sigma_1\xi R - (\mu_c + \vartheta_{cm} + \lambda_c)S_c, \\ S_m' &= \vartheta_{cm}S_c(1-\sigma_1-\sigma_2)\xi R - (\mu_m + \vartheta_{ma} + \lambda_m)S_m, \\ S_a' &= \vartheta_{ma}S_m + \sigma_2\xi R - (\mu_a + \lambda_a)S_a, \\ E_c' &= \lambda_c S_c - (\mu_c + \tau_c)E_c, \\ E_m' &= \lambda_m S_m - (\mu_m + \tau_m)E_m, \\ E_a' &= \lambda_a S_a - (\mu_a + \tau_a)E_a, \\ I_c' &= \tau_c E_c - (\mu_c + d_c + \alpha_c)I_c, \\ I_m' &= \tau_m E_m - (\mu_m + d_m + \alpha_m)I_m, \\ I_a' &= \tau_a E_a - (\mu_a + d_a + \alpha_a)I_a, \\ T' &= \alpha_c I_c + \alpha_m I_m + \alpha_a I_a - (\mu_h + \gamma_h)T, \\ R' &= \gamma_h T - (\mu_h + \xi)R, \end{cases} \tag{1}$$

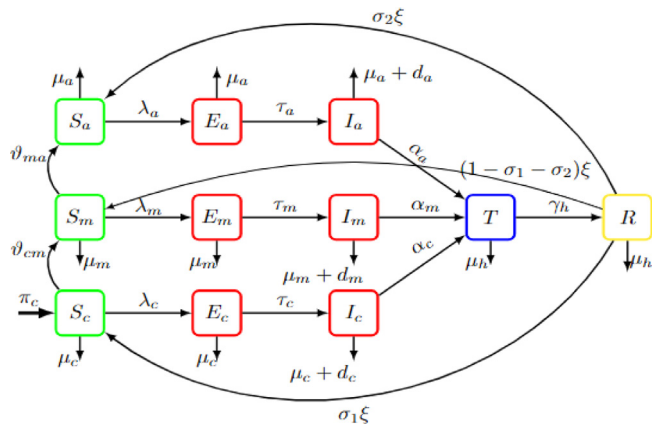

Fig. 1. Model diagram for pneumonia transmission with three age sub-populations.

with positive initial conditions

$S_i(0) > 0, E_i(0) \geq 0, I_i(0) \geq 0, T(0) \geq 0, R(0) \geq 0.$

3. Mathematical analysis

3.1. Invariant region, well-posedness and boundedness of solutions

The invariant region, well-posedness, non-negativity, and boundedness of solutions of the proposed model can be shown using the basic theory of dynamical systems as described in [27–29]. The solutions with non-negative initial conditions remain in a neighborhood of the closed positive hyperspace, $\mathbb{R}^{11}_+$, over the modeling time, that is, $(S_i, E_i, I_i, T, R) \in \mathbb{R}^{11}_+$, since

$$\begin{aligned}
&T'|_{T=0} = (\alpha_c I_c + \alpha_m I_m + \alpha_a I_a) \geq 0, \quad R'|_{R=0} = \gamma_h T \geq 0,\\
&E'_c|_{E_c=0} = \lambda_c S_c \geq 0, \ E'_m|_{E_m=0} = \lambda_m S_m \geq 0, \ E'_a|_{E_a=0} = \lambda_a S_a \geq 0,\\
&I'_c|_{I_c=0} = \tau_c E_c \geq 0, \ I'_m|_{I_m=0} = \tau_m E_m \geq 0, \ I'_a|_{I_a=0} = \tau_a E_a \geq 0,\\
&S'_c|_{S_c=0} = \pi_c + \sigma_1 \xi R \geq 0, \quad S'_m|_{S_m=0} = \vartheta_{cm} + (1-\sigma_1-\sigma_2)\xi R \geq 0,\\
&S'_a|_{S_a=0} = \vartheta_{ma} + \sigma_2 \xi R \geq 0.
\end{aligned} \tag{2}$$

Adding all the equations of the system, we obtain the following dynamic of the total population $N' = \pi_c - \mu_c N_c - \mu_m N_m - \mu_a N_a - \mu_h(T + R) - d_c I_c - d_m I_m - d_a I_a$ where $N_i = S_i + E_i + I_i, \ i \in \{c, m, a\}$. Knowing that μ_c is less than μ_h, μ_m and μ_a. We obtain the following differential inequality, $N'(t) \leq \pi_c - \mu_c N_h$ whose solutions is

$$N(t) \leq \frac{\pi_c}{\mu_h} + \left(N(0) - \frac{\pi_c}{\mu_c}\right) e^{-\mu_c t}.$$

Thus, it follows using the theory of differential inequalities, the biologically feasible region for Model (1) is defined as Ω_h satisfies

$$\Omega_h = \left\{(S_i, E_i, I_i, T, R) \in \mathbb{R}^{11}_+ \ : \ N_h \leq \frac{\pi_c}{\mu_c}\right\},$$

and is positively invariant and attracting in the defined feasible region, Ω_h. Note that the inequalities in (2) implies the region Ω_h is positively invariant for system (1). Thus, for any initial conditions in Ω_h; the solution trajectories will remain in Ω for all time, t. Using a standard method (See, for instance, [27]), we can show that for any initial conditions in Ω_h, there exists a unique solution of system (1) in Ω_h for $t \in [0, \infty)$. Therefore, Model (1) is epidemiologically and mathematically well-posed.

3.2. Disease-free equilibrium and the basic reproduction number

Theorem 1. *The disease-free equilibrium (DFE) of Model (1) is given by*

$$\begin{aligned}
\mathcal{E}^0 &= (S_i^0, E_i^0, I_i^0, T^0, R^0),\\
&= \left(\frac{\pi_c}{(\mu_c + \vartheta_{cm})}, \frac{\pi_c \vartheta_{cm}}{(\mu_c + \vartheta_{cm})(\mu_m + \vartheta_{ma})}, \frac{\pi_c \vartheta_{cm} \vartheta_{ma}}{\mu_a(\mu_c + \vartheta_{cm})(\mu_m + \vartheta_{ma})},\right.\\
&\quad \left. 0, 0, 0, 0, 0, 0, 0, 0\right).
\end{aligned}$$

For simplicity sake, we shall let $g_1 = (\mu_c + \tau_c)$, $g_2 = (\mu_m + \tau_m)$, $g_3 = (\mu_a + \tau_a), g_4 = (\mu_c + d_c + \alpha_c)$, $g_5 = (\mu_m + d_m + \alpha_m)$, $g_6 = (\mu_a + d_a + \alpha_a)$, $g_7 = (\mu_h + \gamma_h)$ and $g_8 = (\mu_h + \xi)$ throughout the rest of the paper.

To compute the basic reproduction number ($\mathcal{R}_0^{basic}$), we use the method in [30], which entails determining the transition/transfer matrices F and V as well as the spectral radius of FV^{-1}. Grouping the compartments of the infected individuals of System (1) and decomposing the right-hand-side as $\mathcal{F} - \mathcal{V}$, where $\mathcal{F}$ is the transmission part, we then express the generation of new infections and $\mathcal{V}$ the transition matrix. Therefore, we obtain

$$\mathcal{F} = \begin{pmatrix} \lambda_c S_c \\ \lambda_m S_m \\ \lambda_a S_a \\ 0 \\ 0 \\ 0 \end{pmatrix} \text{ and } \mathcal{V} = \begin{pmatrix} g_1 E_c \\ g_2 E_m \\ g_3 E_a \\ -\tau_c E_c + g_4 I_c \\ -\tau_m E_m + g_5 I_m \\ -\tau_a E_a + g_6 I_a \end{pmatrix}.$$

Thus,

$$F = \begin{pmatrix} 0 & 0 & 0 & \frac{\beta_c S_c^0}{N^0} & \frac{\beta_c \eta S_c^0}{N^0} & \frac{\beta_c S_c^0}{N^0} \\ 0 & 0 & 0 & \frac{\beta_m S_m^0}{N^0} & \frac{\beta_m \eta S_m^0}{N^0} & \frac{\beta_m S_m^0}{N^0} \\ 0 & 0 & 0 & \frac{\beta_a S_a^0}{N^0} & \frac{\beta_a \eta S_a^0}{N^0} & \frac{\beta_a S_a^0}{N^0} \\ 0 & 0 & 0 & 0 & 0 & 0 \\ 0 & 0 & 0 & 0 & 0 & 0 \\ 0 & 0 & 0 & 0 & 0 & 0 \end{pmatrix}$$

and $V = \begin{pmatrix} g_1 & 0 & 0 & 0 & 0 & 0 \\ 0 & g_2 & 0 & 0 & 0 & 0 \\ 0 & 0 & g_3 & 0 & 0 & 0 \\ -\tau_c & 0 & 0 & g_4 & 0 & 0 \\ 0 & -\tau_m & 0 & 0 & g_5 & 0 \\ 0 & 0 & -\tau_a & 0 & 0 & g_6 \end{pmatrix}.$

Re-defining $\mathcal{A}_1 = \frac{S_c^0}{N^0}$, $\mathcal{A}_2 = \frac{S_m^0}{N^0}$, $\mathcal{A}_3 = \frac{S_a^0}{N^0}$ and computing FV^{-1} we have that and

$$FV^{-1} = \begin{pmatrix} \frac{\beta_c \mathcal{A}_1 \tau_c}{g_1 g_4} & \frac{\beta_c \mathcal{A}_1 \eta \tau_m}{g_2 g_5} & \frac{\beta_c \mathcal{A}_1 \tau_a}{g_3 g_6} & \frac{\beta_c \mathcal{A}_1}{g_4} & \frac{\beta_c \mathcal{A}_1 \eta}{g_5} & \frac{\beta_c \mathcal{A}_1}{g_6} \\ \frac{\beta_m \mathcal{A}_2 \tau_c}{g_1 g_4} & \frac{\beta_m \mathcal{A}_2 \tau_m \eta}{g_2 g_5} & \frac{\beta_m \mathcal{A}_2 \tau_a}{g_3 g_6} & \frac{\beta_m \mathcal{A}_2}{g_4} & \frac{\beta_m \mathcal{A}_2 \eta}{g_5} & \frac{\beta_m \mathcal{A}_2}{g_6} \\ \frac{\beta_a \mathcal{A}_3 \tau_c}{g_1 g_4} & \frac{\beta_a \mathcal{A}_3 \tau_m \eta}{g_2 g_5} & \frac{\beta_a \mathcal{A}_3 \tau_a}{g_3 g_6} & \frac{\beta_a \mathcal{A}_3}{g_4} & \frac{\beta_a \mathcal{A}_3 \eta}{g_5} & \frac{\beta_a \mathcal{A}_3}{g_6} \\ 0 & 0 & 0 & 0 & 0 & 0 \\ 0 & 0 & 0 & 0 & 0 & 0 \\ 0 & 0 & 0 & 0 & 0 & 0 \end{pmatrix}. \tag{3}$$

The eigenvalues of the Matrix (3) yields an eigenvalues whose spectral radius is the pneumonia basic reproduction number is given by

$$\mathcal{R}_0^{basic} = \mathcal{R}_0^{I_c} + \mathcal{R}_0^{I_m} + \mathcal{R}_0^{I_a},$$

where

$$\mathcal{R}_0^{I_c} = \frac{\beta_c \tau_c \mathcal{A}_1}{g_1 g_4}, \quad \mathcal{R}_0^{I_m} = \frac{\beta_m \tau_m \eta \mathcal{A}_2}{g_2 g_5}, \quad \text{and} \quad \mathcal{R}_0^{I_a} = \frac{\beta_a \tau_a \mathcal{A}_3}{g_3 g_6}. \tag{4}$$

Remark 1. We have the following remarks:

(a) The terms contained in $\mathcal{R}_0^{basic}$ represent the direct and indirect transmission pathways between the three subgroups.
(b) The term $\mathcal{R}_0^{I_c}$, $\mathcal{R}_0^{I_m}$ and $\mathcal{R}_0^{I_a}$ in (4) is the contribution that results from the interactions among the sub-populations when an infectious individual is introduced into the human population for the I_c, I_m and I_a the infectious classes for those above 65, between 5 and 64, and children under the age of 5, respectively.

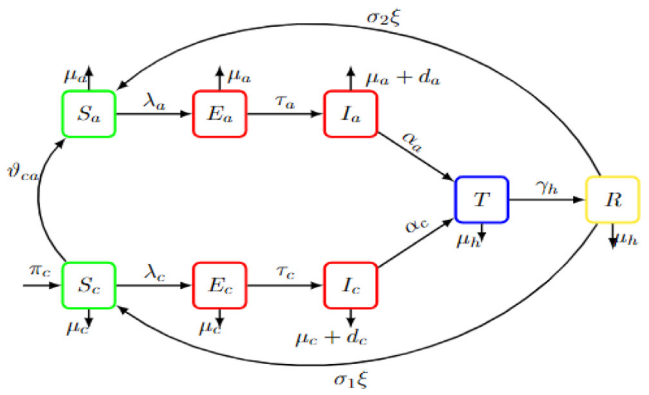

Fig. 2. Model diagram for pneumonia transmission for high-risk sub-population only.

3.3. Model for high-risk group only

Setting the transmission rates (that is, $\lambda_m = \vartheta_{cm} = \eta = \tau_m = \alpha_m = 0$) for those in the sub-group between 5 and 64 and adults over 65 years yields a sub-model for those at high risk of infection. Model diagram 1 reduces to Fig. 2 with the forces of infections for the high-risk subpopulation being λ_c and λ_a.

High-risk basic reproduction number: The basic reproduction number for the high-risk population, $\mathcal{R}_0^{risk}$, is also computed by using the methodology in we use the method in [30] and found to be

$$\mathcal{R}_0^{risk} = \underbrace{\left\{\frac{\beta_a \mathcal{A}_3 \tau_a}{g_3 g_6} + \frac{\beta_c \mathcal{A}_1 \tau_c}{g_1 g_4}\right\}}_{\text{effect of high-risk transmission}}.$$

Remark 2. Clearly, $\mathcal{R}_0^{risk} \subset \mathcal{R}_0^{basic}$, but one cannot predict if it increases the numerical value of $\mathcal{R}_0^{risk}$ which drives the infection in the whole population.

3.4. Global stability of the disease-free equilibrium

To prove the global asymptotically stability (GAS) of the DFE, we use the approach as described in [31]. We then re-write the pneumonia model (1) as follows:

$$\begin{cases} \dfrac{dX}{dt} &= F(X, I), \\ \dfrac{dI}{dt} &= \mathcal{G}(X, I), \quad \mathcal{G}(X, 0) = 0, \end{cases} \tag{5}$$

in which $X = (S_c, S_m, S_a, T, R) \in \mathbb{R}^5$ and $I = (E_c, E_m, E_a, I_c, I_m, I_a) \in \mathbb{R}^6$. Note that X and I represent the classes of the un-infectious and infectious individuals, respectively. For the model to be GAS at $\mathcal{E}^0$, it needs to satisfy the following conditions as adopted from [31], which are

- (C_1) Local stability is guaranteed at $\mathcal{E}^0$ whenever $\mathcal{R}_0 < 1$.
- (C_2) At $\dfrac{dX}{dt} = F(X_0, 0)$ the DFE is globally asymptotically stable.
- (C_3) $\mathcal{G}(X, I) = \mathcal{A}I - \hat{\mathcal{G}}(X, I)$, $\hat{\mathcal{G}}(X, I) \geq 0$ for $(X, I) \in \Omega$, where $X_0 = \mathcal{E}^0$,
  $\mathcal{A} = \mathcal{D}_I \mathcal{G}(\mathcal{E}^0)$ is a Metzler matrix, and Ω is the model biologically feasible region defined earlier.

Theorem 2. *Let $t > 0$, if $S_i^0 N(t) > S_i(t) N^0$ for all $i \in \{a, c, m\}$, then The disease-free equilibrium $\mathcal{E}^0$ is GAS stable when $\mathcal{R}_0^{basic} < 1$.*

Proof. To prove that the DFE is GAS when $\mathcal{R}_0^{basic} < 1$, we have to verify the conditions C_1 to C_3. Using the result in [30], we obtain that the DFE $\mathcal{E}^0$ is LAS when $\mathcal{R}_0 < 1$, so the condition C_1 is verified. Next, we re-write the model system (1) in the form given in (5) as

$$\frac{dX}{dt} = F(X, I) = \begin{pmatrix} \pi_c + \sigma_1 \xi R - (\mu_c + \vartheta_{cm} + \lambda_c) S_c \\ \vartheta_{cm} S_c + \sigma_2 \xi R - (\mu_m + \vartheta_{ma} + \lambda_m) S_m \\ \vartheta_{ma} S_m + (1 - \sigma_1 - \sigma_2) \xi R - (\mu_a + \lambda_a) S_a \\ \alpha_c I_c + \alpha_m I_m + \alpha_a I_a - (\mu_h + \gamma) T \\ \gamma T - (\mu_h + \xi) R \end{pmatrix} \tag{6}$$

and

$$\frac{dI}{dt} = G(X, I) = \begin{pmatrix} \lambda_c S_c - g_1 E_c \\ \lambda_m S_m - g_2 E_m \\ \lambda_a S_a - g_3 E_a \\ \tau_c E_c - g_4 I_c \\ \tau_c E_m - g_5 I_m \\ \tau_a E_a - g_6 I_a \end{pmatrix}. \tag{7}$$

We have that

$$\frac{dX}{dt} = F(X_0, 0) \Leftrightarrow \begin{cases} S_c' = \pi_c + \sigma_1 \xi R - (\mu_c + \vartheta_{cm} + \lambda_c) S_c, \\ S_m' = \vartheta_{cm} S_c + \sigma_2 \xi R - (\mu_m + \vartheta_{ma}) S_m, \\ S_a' = \vartheta_{ma} S_m + (1 - \sigma_1 - \sigma_2) \xi R - (\mu_a + \lambda_a) S_a, \\ T' = -(\mu_h + \gamma) T, \\ R' = \gamma T - (\mu_h + \xi) R. \end{cases} \tag{8}$$

This equation has a unique equilibrium point:

$$\left(\frac{\pi_c}{(\mu_c + \vartheta_{cm})}, \frac{\pi_c \vartheta_{cm}}{(\mu_c + \vartheta_{cm})(\mu_m + \vartheta_{ma})}, \frac{\pi_c \vartheta_{cm} \vartheta_{ma}}{\mu_a (\mu_c + \vartheta_{cm})(\mu_m + \vartheta_{ma})}, 0, 0\right),$$

which is globally asymptotically stable. Therefore, the condition C_2 is satisfied. Linearizing the second matrix in Eqs. (6) and (7) gives the Metzler Matrix

$$\mathcal{A} = \mathcal{D}_Z \mathcal{G}(\mathcal{E}^0) = \begin{pmatrix} -g_1 & 0 & 0 & \frac{\beta_c S_c^0}{N^0} & \frac{\beta_c \eta S_c^0}{N^0} & \frac{\beta_c S_c^0}{N^0} \\ 0 & -g_2 & 0 & \frac{\beta_m S_m^0}{N^0} & \frac{\beta_m \eta S_m^0}{N^0} & \frac{\beta_m S_m^0}{N_h^0} \\ 0 & 0 & -g_3 & \frac{\beta_a S_a^0}{N^0} & \frac{\beta_a \eta S_a^0}{N^0} & \frac{\beta_a S_a^0}{N^0} \\ \tau_c & 0 & 0 & -g_4 & 0 & 0 \\ 0 & \tau_m & 0 & 0 & -g_5 & 0 \\ 0 & 0 & \tau_a & 0 & 0 & -g_6 \end{pmatrix}.$$

Computing $\hat{\mathcal{G}}(X, Z)$ and after some algebraic simplifications, we have

$$\hat{\mathcal{G}}(X, I) = \mathcal{A}I - \mathcal{G}(X, I) = \begin{pmatrix} \beta_c (I_c + \eta I_m + I_a) \left[\dfrac{S_c^0}{N^0} - \dfrac{S_c}{N}\right] \\ \beta_m (I_c + \eta I_m + I_a) \left[\dfrac{S_m^0}{N^0} - \dfrac{S_m}{N}\right] \\ \beta_a (I_c + \eta I_m + I_a) \left[\dfrac{S_a^0}{N^0} - \dfrac{S_a}{N}\right] \\ 0 \\ 0 \\ 0 \end{pmatrix}.$$

Thus,

$$\hat{\mathcal{G}}(X, I) = \begin{pmatrix} \beta_c (I_c + \eta I_m + I_a) \left[\dfrac{N S_c^0 - S_c N^0}{N N^0}\right] \\ \beta_m (I_c + \eta I_m + I_a) \left[\dfrac{S_m^0 N - S_m N^0}{N N^0}\right] \\ \beta_a (I_c + \eta I_m + I_a) \left[\dfrac{S_a^0 N - S_a N^0}{N N^0}\right] \\ 0 \\ 0 \\ 0 \end{pmatrix}.$$

Table 2
Parameters values for the population under 5 years.

Parameters	Range	Baseline value	Ref.
π_c	1–10,687	100	[35]
β_c		0.12675	Assumed
τ_c	$\left[\frac{1}{6}-\frac{1}{4}\right]$	0.2	[36]
α_c	$\left[\frac{1}{7}-\frac{1}{4\times7}\right]$	$\frac{1}{3\times7}$	[37]
d_c	0.00121–0.00363	0.00360	[38]
μ_c	–	$\frac{5.4}{1000\times365}$	[34]
σ_1	(0,1)	0.55	Assumed

Table 3
Parameters values for the population between the ages of 5 and 64 years.

Parameters	Range	Baseline value	Ref.
μ_m	$\left(\frac{1}{74\times365}-\frac{1}{15\times365}\right)$	$\frac{1}{55.5\times365}$	Assumed
β_m		0.1028	Assumed
τ_m	(0,1)	0.5	[24]
α_m	(0,1)	0.03	Assumed
d_m	0.001–0.002	0.002	[38]
σ_2	(0-1)	0.35	Assumed
η	(0,1)	0.895	Varied
ϑ_{cm}	–	$\frac{1}{5\times365}$	Estimated

Table 4
Parameters values for adult population above 65 years.

Parameters	Range	Baseline value	Ref.
μ_a	$\left(\frac{1}{25\times365}-\frac{1}{14\times365}\right)$	$\frac{1}{20\times365}$	Assumed
β_a		0.1379	Assumed
τ_a	(0,1)	0.590313	[21,24]
α_a	(0,1)	0.025	Assumed
d_a	(0,1)	0.00264	[38]
ϑ_{ma}	–	$\frac{1}{58\times365}$	Estimated
μ_h	–	$\frac{1}{76.4\times365}$	[32]
γ_h	$\left[\frac{1}{4\times7},\frac{1}{2\times7}\right]$	$\frac{1}{4\times7}$	[33]
ξ	(0,1)	0.07	[24]

Because $S_a^0N-S_aN^0$, $S_a^0N-S_aN^0$ and $S_a^0N-S_aN^0$ are all positives due to our assumption, we obtain $\hat{\mathcal{G}}(X,I)\geq 0$. The condition C_3 is satisfied. We can conclude that if $S_i^0N > S_iN^0$ for all $i\in\{a,c,m\}$ then, the DFE is GAS when $\mathcal{R}_0^{basic}<1$. The proof ends here, and the numerical simulation is presented in the next section. □

4. Numerical simulations

In this section, we present some numerical simulation, which involves solving our model numerically using Matlab software. This helps to simulate inherent dynamics and the influence of certain parameters on Model (1). First, we parametrize our model using available parameters from the literature that modeled or portray infection rates for pneumonia in the human population following available epidemiological data on the disease.

4.1. Parametrization

We parametrize our model by using the available parameter values from published literature reflecting the actual transmission rates as we defined in our model formulation. In the event parameters are not found in the literature, it was assumed as indicated. In particular, Table 4 gives the parameter values for adults over 65, Table 3 shows parameter values for the population between the ages of 5 and 64, and Table 2 shows that of the population under the ages of 5. The parameter values in commons for the three sub-populations, which are μ_h,γ_h and ξ were parametrized as follows; we assumed a general mortality rate of $\mu_h=\frac{1}{76.4\times365}\text{day}^{-1}$ for all populations taken from [32] and used a recovery period of Pneumonia, which is between 2 to 4 weeks hence, we set $\gamma_h=\left[\frac{1}{4\times7},\frac{1}{2\times7}\right]\text{day}^{-1}$ [33]. Additionally, we assign the loose immunity rate, $\xi=0.07$, implied from [24]. Knowing that the respective time spent in days in the population aged under 5 and in the population aged between 5 and 64 is 5×365 and 58×365, respectively, we set the maturation parameters from the population under 5 to the population aged 5 to 64 and from the latter to the population aged over 65 to $\vartheta_{cm}=\frac{1}{5\times365}\ \text{day}^{-1}$ and $\vartheta_{ma}=\frac{1}{58\times365}\ \text{day}^{-1}$. Regarding the values of the different natural mortality, the one of the population under 5 years is $\mu_c=\frac{5.4}{1000\times365}\ \text{day}^{-1}$[34], we assumed that $\mu_m=\frac{1}{55.5\times365}\ \text{day}^{-1}$ and $\mu_a=\frac{1}{20\times365}\ \text{day}^{-1}$. The remaining parameters are taken from published literature, taking into account the epidemiological characteristics/features of Pneumonia infection as referenced and summarized in Tables 2, 3 and 4.

4.2. Convergence of endemic equilibrium

The existence of an endemic equilibrium which reflects an endemicity of infection or persistence of the disease is graphically presented in Fig. 3 by numerically simulating Model (1) for given initial conditions in Table 5 given in the Appendix. Fig. 3 depicts the existence of an endemic equilibrium when $\mathcal{R}_0^{basic}$ is above one ($\mathcal{R}_0^{basic}=1.94$). It can be observed from Fig. 3 that starting with any different sets of initial conditions (number of individuals) the model solution will always converge to a stable equilibrium point for compartments: S_a versus E_a, E_a versus I_a, S_c versus I_c, S_m versus I_m in Figs. 3(a), 3(b), 3(c) and 3(d) respectively. Similarly, the results shown in Figure can be obtained for the combination of the rest state variables T, R, E_m and E_c. Thus, we have numerically shown that our model will exhibit a unique endemic equilibrium.

4.3. Global sensitivity analysis

In general, mathematical models have some uncertainties that could result from the inherent dynamics of the model or from parametrization, which adopts its numerical values from available epidemiological or demographic parameters. Additionally, the parameter values are based on simplifying assumptions representing real-life scenarios and cannot completely replicate the inherent complexity of the entire system. Consequently, there are usually errors in data collection and presumed parameter values [39]. For this reason, sensitivity analysis is commonly used to determine the robustness of the model predictions to parameter values [39]. We employ the Partial Rank Correlation Coefficients (PRCC's) and the Latin Hypercube Sampling (LHS) [39], to identify model parameters that have a high impact on the initial disease prevalence using the high-risk infectious state variables as a response function. Model (1) is simulated in Matlab with 1000 runs, unit step size of 1, and for over 60 days with a uniform distribution while sampling the parameters and the results are presented in Figs. 4(a) and 4(b) using (I_a+I_c) and $(I_a+I_c+I_m)$ as response functions respectively. We aim to use all the model parameters besides recruitment and death rates to determine their variability in the transmissibility rate of pneumonia infections considering the subject under investigation while focusing on the population at high risk of infection. The magnitude, as well as the direction of the PRCC values for distinct parameters, are of primary importance in determining the contribution of a respective parameter to the model prediction and level of accuracy. Thus, PRCC values higher than 0.5 (closer to 1) and lower than −0.5 (closer to

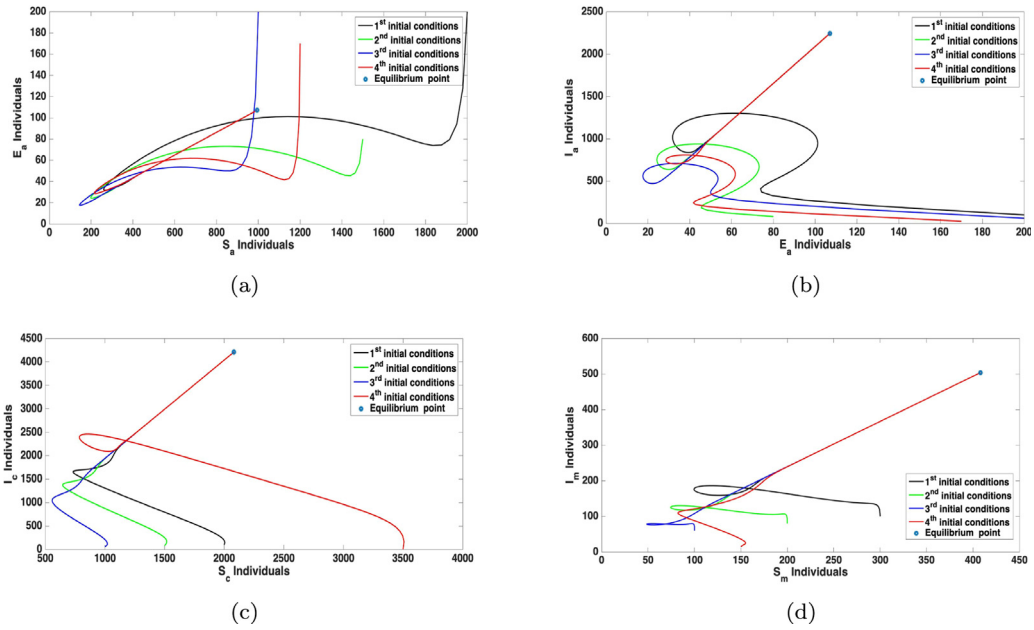

Fig. 3. Plots showing the existence of endemic equilibrium using parameters defined in Tables 2–4 and different sets of initial conditions in Table 5 for: (a) S_a versus E_a, (b) E_a versus I_a, (c) S_c versus I_c and S_m versus I_m when $\mathcal{R}_0^{basic} = 1.94 > 1$.

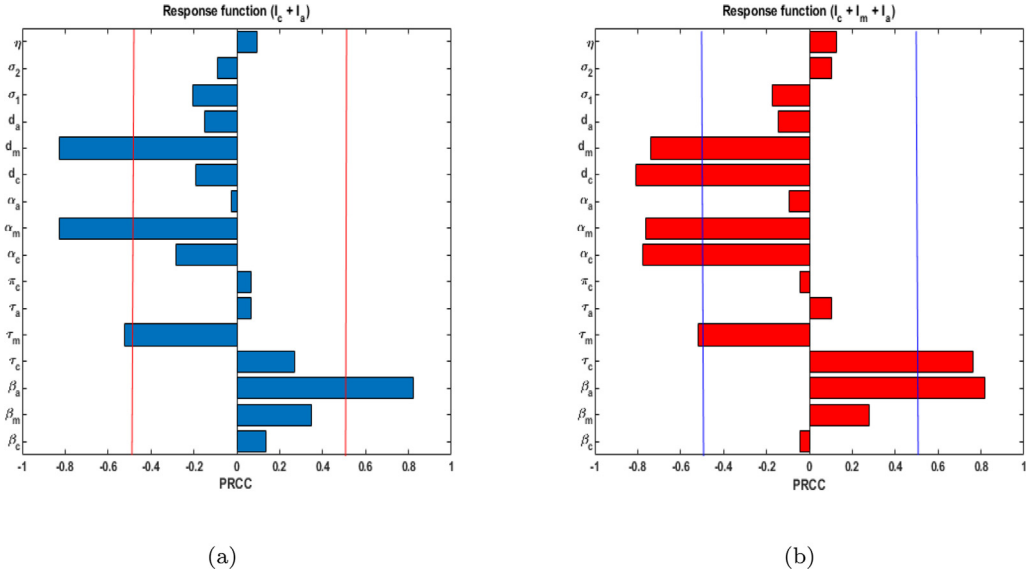

Fig. 4. Tornado plot showing PRCC's values for model parameters excluding ϑ_{cm}, ϑ_{ma} and μ_i for $i = h, a, c, m$ against (a) $(I_a + I_c)$ and (b) $(I_a + I_m + I_c)$ as a response functions.

-1) are quite important, as this implies a stronger influence of the LHS parameter on the outcome measure. In Figs. 4(a) and 4(b), we clearly notice that the parameters $\beta_m, \beta_a, \tau_c, \tau_m, \alpha_c, \alpha_m, d_c$ and d_m have a stronger influence on the infected populations considered. It is clearly observed that the contact rate (β_m) has PRCC values very close to 1 for the two populations of infected considered and the contact rate β_a has PRCC values very close to 1 for $(I_c + I_m + I_a)$ (Fig. 4(b)), which means a higher level of uncertainties or variations of the infected population $(I_c + I_m + I_a)$ (Fig. 4(b)) and $(I_c + I_a)$ (Fig. 4(a)) with a change of its values. The fact that the PRCC is closer to 1 which means a strong positive correlation. We observe that the rates τ_m, α_c and α_m have negative PRCC values, thus signifying the crucial role of the treatments. Thus, for public health concerns, the leaders should seek to implement control strategies that target reducing the effective transmission rates among adults over 65, modification parameters for infectious humans under 5, and progression rates for those between 5 and 64. See [40–46] for similar analyses on other epidemic modeling works in literature and their findings.

4.4. Impact of treatment rates and η on infected populations

We carried out a numerical simulation to investigate the impact of treatment rates (α_a, α_c and α_m) on pneumonia-infected total populations by using the same treatment rates, that is, $\alpha_a = \alpha_c = \alpha_m = 0.025, 0.035, 0.045, 0.055$ over a long duration of 3000 days. The simulation results are presented in Fig. 5. It is observed in Figs. 5(a) and 5(c) that with the same rate of treatments, we have a greater reduction in infected humans when varying α_c and α_a or implementing different rate of treatments as time progress. In contrast, using the same equation amount of treatment rates yields fewer effects on reducing the total number of infectious individuals, as shown in Fig. 5(b) over the modeling time. Also, we varied the I_m modification parameter (η) on

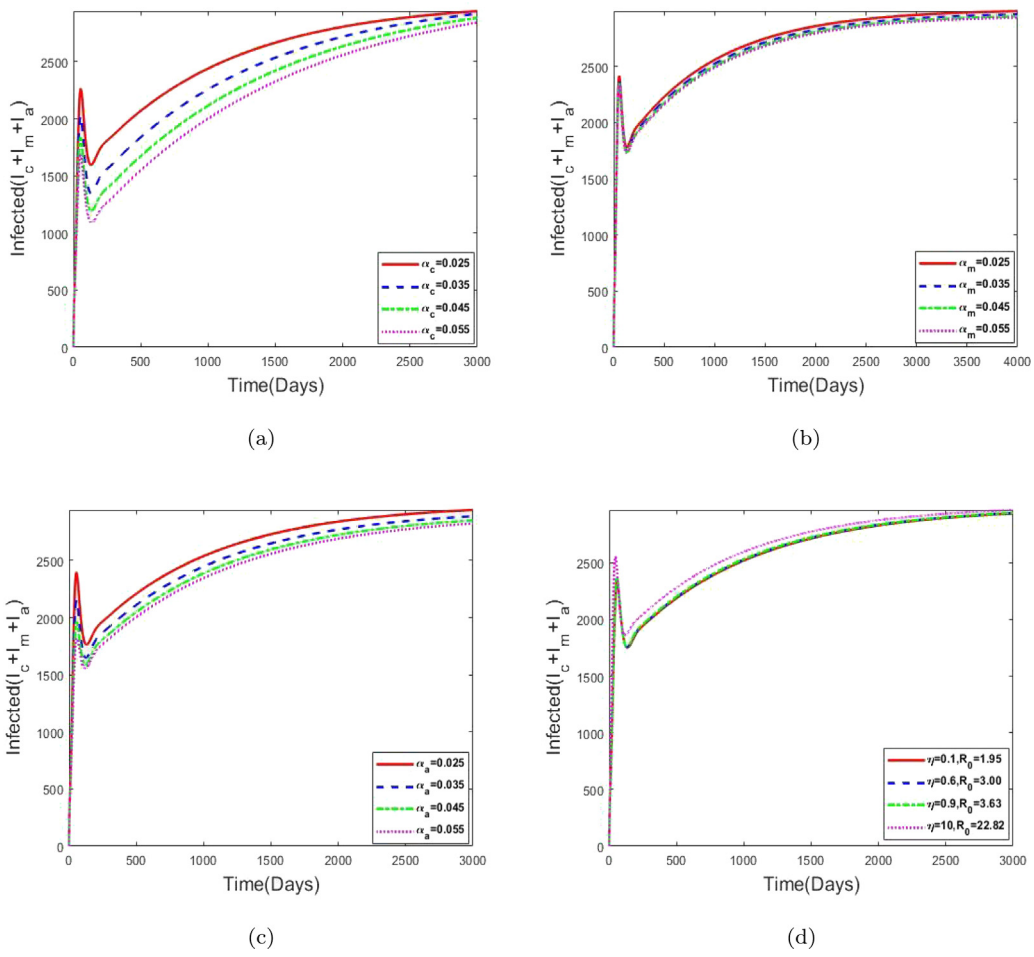

Fig. 5. Varying treatment rates on the total infected population $(I_a + I_c + I_m)$ for: (a) α_c, (b) α_m (c) α_a and (d) η. The rest parameters are kept constant as defined in Tables 2–4.

the total infectious populations, and results show that increasing the parameter leads to more individuals getting infected with pneumonia and the numerical value of the basic reproduction number. Therefore, we state that individuals above and below years also play a crucial role in driving the infections even though we have children under 5 and the elderly above 64 are the high-risk population mostly affected with Pneumonia. Note that, $\mathcal{R}_0^{basic}$ is represented by R_0 in our simulation results.

4.5. Effects of parameters on subgroup pneumonia $\mathcal{R}_0^{basic}$ dynamics

Here, we simulate the impact of the following parameters; high-risk infection rates (β_a, β_c and β_m), and the I_m modification parameter η on the basic reproduction number ($\mathcal{R}_0^{basic}$). The numerical results as 2d plots contour plots with our chosen parameters as a function of $\mathcal{R}_0^{basic}$ obtained are presented in Fig. 6. From Figs. 6(a) and 6(b), we observe that for each of these simulations, the increase in the transmission rates β_a and β_m increases the basic reproduction number for the 2d plot (see Fig. 6(a)). In similar manner, increasing the η and β_m, also leads to increase in the numerical value of $\mathcal{R}_0^{basic}$ as seen in the 2d plot Fig. 6(b). A biological implication of these results signifies that efforts need to be implemented, which should drive effective preventative measures (such as humans practicing proper hygiene and public health educational campaigns, etc.) to reduce transmission rates that cause pneumonia infections in these high-risk groups. At the same time, reducing infection in those individuals above 5 years and younger than 64 years even though they are not termed as high risk of contracting pneumonia infection.

4.6. Varying effective contact rates on infected population

In Fig. 7, we investigated the effect of varying contact rates β_a, β_c and β_m on the sum of the total infectious population $(I_a + I_c + I_m)$. It is observed in Figs. 7(a), 7(b) and 7(c) that increasing the respective contact rates on infected population increases both the basic reproduction number ($\mathcal{R}_0^{basic}$) and the number of infected individual's $(I_a + I_c + I_m)$ over time. A comparison of the results seen in Figs. 7(a), 7(b) and 7(c) shows that varying the contact rates β_c and β_c have more significant impact (see Figs. 7(a) and 7(b)) than when compared to β_m on $(I_a + I_c + I_m)$ respectively (see Fig. 7(c)). This implies that more infectious humans with pneumonia can lead to a high spread of the disease since it reaches its endemicity. Efforts to mitigate the spread of pneumonia and reduce disease transmission by implementing possible control measures to inhibit the spread of Streptococcus pneumonia, focusing more on the high-risk population, that is children under 5 and the elderly over 64 years.

5. Discussion and conclusion

5.1. Strengths, limitations, and comparison with existing studies

One of the strengths of our model is that it subdivides the human population into three high-risk groups, unlike in existing literature, where pneumonia dynamics are generalized across all age groups. Also, our results predict that an effective control strategy, such as treatment at the onset of infection, is vital for mitigating the spread and control of pneumonia within the population.

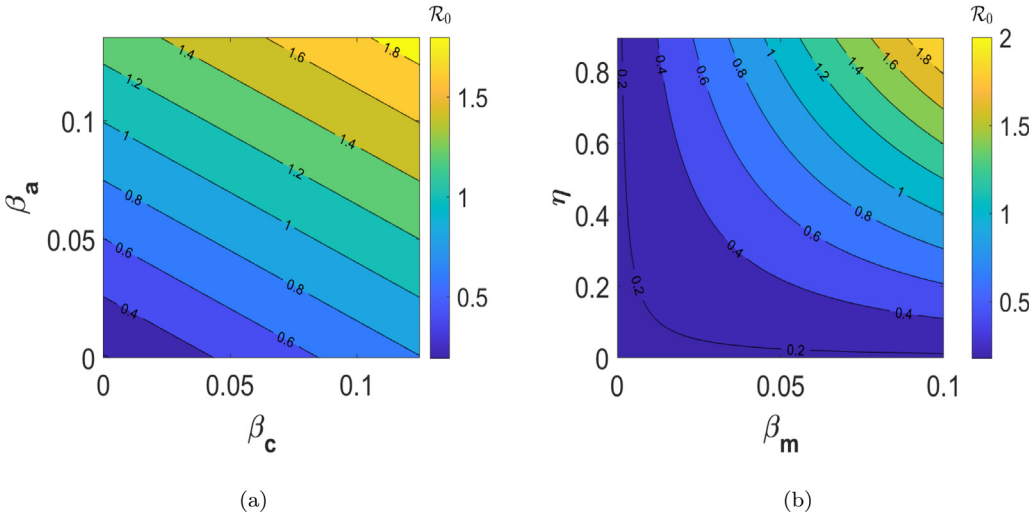

Fig. 6. (a) Contour plot showing the impact of parameters β_a versus β_c on $\mathcal{R}_0$. (b) Contour plot showing the impact of parameters η versus β_m on $\mathcal{R}_0$. The parameter values are varied in the ranges shown in Fig. 6 while the rest parameters are kept constant as defined in Tables 2–4.

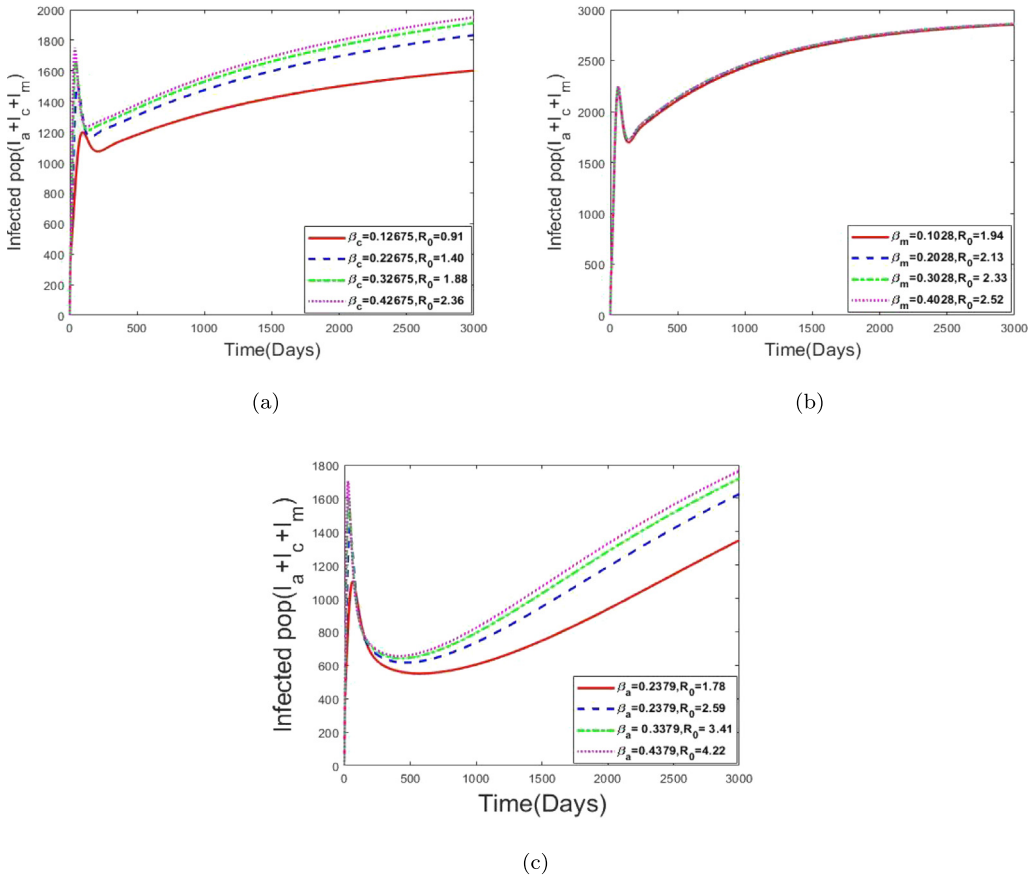

Fig. 7. (a) Varying β_a on the total infected population $(I_a + I_c + I_m)$. (b) Varying β_c on the total infected population $(I_a + I_c + I_m)$. (c) Varying β_m on the total infected population $(I_a + I_c + I_m)$. The parameter values varied are shown in the legend while the rest of the parameters are kept constant as defined in Tables 2–4.

We acknowledge that our model has some shortfalls. First, our model was not fitted to any epidemiological data, and hence, the model parameter values were obtained from literature on pneumonia dynamics reflecting its transmission rates within the human population. In addition, where parameter values were unavailable, we estimated the parameter which gives the endemic equilibrium. However, to encompass this complexity, we carried out a sensitivity analysis that allows for identifying model parameters driving the variability of an epidemic model within a specified range. Last, we assume all individuals in each sup-population progress into the treatment class at different rates.

Notwithstanding these shortfalls, we maintain that our modeling framework remains applicable in controlling and the fight against the elimination of pneumonia, especially among the high-risk population. Our model is comparable to a few existing modeling frameworks in literature for pneumonia infection, such as [3,15,17]. These models analyzed the dynamics of pneumonia among children under the age of 5 years and incorporated treatment and vaccination.

5.2. Concluding remarks

Mathematical modeling helps to improve the understanding of disease evolution and predict effective control strategies required to mitigate the spread of infectious and non-infectious diseases. This paper analyzed a deterministic model for the transmission dynamics of pneumonia among high-risk groups.

Our model categorized humans into three subgroups: children under the age of 5, those between the ages of 5 and 64, and individuals above 65. Mathematical analyses were carried out, and numerical simulations were presented. Simulation results suggest that early treatment could reduce the burden caused by pneumonia infection. As illustrated in Figs. 5 and 7, we recommend that interventions introduced within the community to mitigate the spread of pneumonia should be targeted at reducing the contact rates (β_a, β_c) while increasing the treatment rates (α_c and α_a) of those under 5 and population over age 64 years. Implementing such a strategy could potentially lead to eliminating pneumonia within the community. Complete eradication of the disease will require greater global and concerted efforts to achieve the WHO 2025 target.

Future work can look into developing an aged-structured model that includes time-dependent controls to establish the control measures and cost of implementing controls to help eliminate pneumonia within high-risk groups. Also, we intend to study a multi-scale dynamics of pneumonia-coronavirus disease (COVID-19) co-dynamics to investigate the impact of COVID-19 on the spread of pneumonia infection.

Declaration of competing interest

The authors declare that they have no known competing financial interests or personal relationships that could have appeared to influence the work reported in this paper.

Data availability

No data was used for the research described in this article.

Acknowledgments

We thank our respective universities and the anonymous reviewers for their valuable comments that helped to strengthen this manuscript. SYT expresses acknowledgment of DSI/NRF SARChI M3B2, Grant No. N00317 for Postdoctoral funding.

Funding

This work is not supported by any funding.

Appendix

The calculation for the high-risk basic reproduction number is presented in Section 3.3.

$$\mathcal{F} = \begin{pmatrix} \lambda_c S_c \\ \lambda_a S_a \\ 0 \\ 0 \end{pmatrix} \text{ and } \mathcal{V} = \begin{pmatrix} g_1 E_c \\ g_3 E_a \\ -\tau_c E_c + g_4 I_c \\ -\tau_a E_a + g_6 I_a \end{pmatrix}.$$

Table 5
Various initial conditions (IC) used to obtain the numerical simulation showing model convergence for endemic equilibrium.

IC	$S_c(0)$	$S_m(0)$	$S_a(0)$	$E_c(0)$	$E_m(0)$	$E_a(0)$	$I_c(0)$	$I_a(0)$	$I_m(0)$	$T(0)$	$R(0)$
1st	2000	300	2000	200	50	200	100	100	100	100	100
2nd	1500	200	1500	150	40	200	80	80	80	80	80
3rd	1000	100	1000	100	30	200	60	60	60	60	60
4th	3500	150	1200	750	10	170	5	15	25	35	50

Thus,

$$F = \begin{pmatrix} 0 & 0 & \frac{\beta_c S_c^0}{N^0} & \frac{\beta_c S_c^0}{N^0} \\ 0 & 0 & \frac{\beta_a S_a^0}{N^0} & \frac{\beta_a S_a^0}{N^0} \\ 0 & 0 & 0 & 0 \\ 0 & 0 & 0 & 0 \end{pmatrix} \quad V = \begin{pmatrix} g_1 & 0 & 0 & 0 \\ 0 & g_3 & 0 & 0 \\ -\tau_c & 0 & g_4 & 0 \\ 0 & -\tau_a & 0 & g_6 \end{pmatrix}.$$

Setting $\mathcal{A}_1 = \frac{S_c^0}{N^0}$, $\mathcal{A}_3 = \frac{S_a^0}{N^0}$ and computing FV^{-1} we have that and

$$FV^{-1} = \begin{pmatrix} \frac{\beta_c \mathcal{A}_1 \tau_c}{g_1 g_4} & \frac{\beta_c \mathcal{A}_1 \tau_a}{g_3 g_6} & \frac{\beta_c \mathcal{A}_1}{g_4} & \frac{\beta_c \mathcal{A}_1}{g_6} \\ \frac{\beta_a \mathcal{A}_3 \tau_c}{g_1 g_4} & \frac{\beta_a \mathcal{A}_3 \tau_a}{g_3 g_6} & \frac{\beta_a \mathcal{A}_3}{g_4} & \frac{\beta_a \mathcal{A}_3}{g_6} \\ 0 & 0 & 0 & 0 \\ 0 & 0 & 0 & 0 \end{pmatrix}.$$

References

[1] Causes of Pneumonia, Centre for Disease Control, 2023, https://www.cdc.gov/pneumonia/causes.html#::text=Common%20causes%20of%20bacterial%20pneumonia,from%20those%20in%20healthcare%20settings. Accessed 03/09/2023.
[2] Risk Factors for Pneumonia, CDC, 2023, https://www.cdc.gov/pneumonia/riskfactors.html#::text=Adults%2065%20years%20or%20older,in%20people%20of%20all%20ages, Accessed 03/07/2023.
[3] M. Kizito, J. Tumwiine, A mathematical model of treatment and vaccination interventions of pneumococcal Pneumonia infection dynamics, J. Appl. Math. 2018 (2018).
[4] G. Regev-Yochay, M. Raz, R. Dagan, et al., Nasopharyngeal carriage of Streptococcus pneumoniae by adults and children in community and family settings, Clin. Infect. Dis. 38 (5) (2004) 632–639.
[5] T. Leino, K. Auranen, J. Jokinen, M. Leinonen, P. Tervonen, A.K. Takala, Pneumococcal carriage in children during their first two years: Important role of family exposure, Te Pediatr. Infect. Dis. J. 20 (11) (2001) 1022–1027.
[6] Pneumonia, WHO, 2023, https://www.who.int/news-room/fact-sheets/detail/pneumonia, Accessed 03/06/2023.
[7] Key Facts, Pneumonia in Children, WHO, 2023, https://www.who.int/news-room/fact-sheets/detail/pneumonia#::text=treat%20pneumonia%20focusing%20on%20making,they%20need%20to%20get%20well, Accessed 03/06/2023.
[8] B.M. Farr, C.L.R. Bartlett, J. Wadsworth, D.L. Miller, Risk factors for community-acquired Pneumonia diagnosed upon hospital admission, Respir. Med. 94 (10) (2000) 954–963.
[9] J.H. Reynolds, G. McDonald, H. Alton, S.B. Gordon, Pneumonia in the immunocompetent patient, Br. J. Radiol. 83 (996) (2010) 998–1009.
[10] C.M.C. Rodrigues, Challenges of empirical antibiotic terapy for community-acquired pneumonia in children, Curr. Terapeutic Res. - Clin. Exp. 84 (2017) e7–e11.
[11] T. Wardlaw, P. Salama, E.W. Johansson, E. Mason, Pneumonia: the leading killer of children, Lancet 368 (9541) (2006) 1048–1050.
[12] D. Otoo, P. Opoku, S. Charles, A.P. Kingsley, Deterministic epidemic model for ($SVCSyCAsyIR$) pneumonia dynamics, with vaccination and temporal immunity, Infect. Dis. Model. 5 (2020) 42–60.
[13] J. Alya, D. Aldila, R. Rusin, A mathematical model of the spread of pneumococcal pneumonia disease by considering vaccine and hospital care interventions, in: AIP Conference Proceedings, Vol. 2498, AIP Publishing, 2022, August, No. 1.
[14] M. Horn, C. Theilacker, R. Sprenger, C. von Eiff, E. Mahar, J. Schiffner-Rohe, M.W. Pletz, M. van der Linden, M. Scholz, Mathematical modeling of pneumococcal transmission dynamics in response to PCV13 infant vaccination in Germany predicts increasing IPD burden due to serotypes included in next-generation PCVs, Plos One 18 (2) (2023) e0281261.
[15] I.K. Oluwatobi, L.M. Erinle-Ibrahim, Mathematical modeling of pneumonia dynamics of children under the age of five, 2021.

[16] M. Kassa, S.N. Murthy, Pneumonia control measures under five year children IOSR, J. Math. 12 (2016) 64–70.
[17] M.J. Ong'ala Jacob Otieno, O. Paul, Mathematical model for Pneumonia dynamics with carriers, Int. J. Math. Anal. 7 (50) (2013) 2457—2473.
[18] M.C. Swai, N. Shaban, T. Marijani, Optimal control in two strain pneumonia transmission dynamics, J. Appl. Math. (2021).
[19] B.S. Kotola, T.T. Mekonnen, Mathematical model analysis and numerical simulation for codynamics of meningitis and pneumonia infection with intervention, Sci. Rep. 12 (1) (2022) 2639.
[20] G.T. Tilahun, O.D. Makinde, D. Malonza, Modelling and optimal control of pneumonia disease with cost-effective strategies, J. Biol. Dyn. 11 (sup2) (2017) 400–426.
[21] D. Aldila, N. Awdinda, F.F. Herdicho, M.Z. Ndii, C.W. Chukwu, Optimal control of pneumonia transmission model with seasonal factor: Learning from Jakarta incidence data, Heliyon (2023).
[22] H. Regunath, Y. Oba, Community-acquired pneumonia, in: StatPearls, StatPearls Publishing, Treasure Island (FL), 2022, https://www.ncbi.nlm.nih.gov/books/NBK430749/, Accessed 03/06/2023.
[23] J. Chastre, M. Wolff, J. Fagon, et al., Comparison of 8 vs 15 days of antibiotic therapy for ventilator-associated pneumonia in adults: A randomized trial, JAMA 290 (19) (2003) 2588—2598.
[24] O.C. Zephaniah, U.I.R. Nwaugonma, I.S. Chioma, O. Andrew, A mathematical model and analysis of an SVEIR model for streptococcus Pneumonia with saturated incidence force of infection, Math. Model. Appl. 5 (1) (2020) 16–38.
[25] M. Naveed, D. Baleanu, A. Raza, M. Rafiq, A.H. Soori, M. Mohsin, Modeling the transmission dynamics of delayed pneumonia-like diseases with a sensitivity of parameters, Adv. Difference Equ. 2021 (1) (2021) 1–19.
[26] M.I. Ossaiugbo, N.I. Okposo, Mathematical modeling and analysis of Pneumonia infection dynamics, Sci. World J. 16 (2) (2021) 73–80.
[27] C.W. Chukwu, F. Nyabadza, Mathematical Modeling of Listeriosis incorporating effects of awareness programs, Math. Models Comput. Simul. 13 (2021) 723–741.
[28] Z. Mukandavire, A.B. Gumel, W. Garira, J.M. Tchuenche, Mathematical analysis of a model for HIV-malaria co-infection, Math. Biosci. Eng. 6 (2) (2009) 333–362.
[29] C.W. Chukwu, F. Nyabadza, Fatmawati, Modelling the potential role of media campaigns on the control of Listeriosis, Math. Biosc. Eng. 18 (6) (2021) 7580–7601.
[30] P. Van den Driessche, J. Watmough, Reproduction numbers and sub-threshold endemic equilibria for compartmental models of disease transmission, Math. Biosci. 180 (1–2) (2002) 29–48.
[31] Carlos Castillo-Chavez, Zhilan Feng, Wenzhang Huang, et al., On the computation of Ro and its role, in: Mathematical Approaches for Emerging and Reemerging Infectious Diseases: an Introduction, Vol. 1, 2002, p. 229.
[32] https://www.macrotrends.net/countries/USA/united-states/life-expectancy, Accessed 03/06/2023.
[33] Pneumonia, National Institute of Health, 2023, https://www.nhs.uk/conditions/pneumonia/, Accessed 03/07/2023.
[34] Statista, Infant mortality in the United States from 2011 to 2021, 2023, https://www.statista.com/statistics/263738/infant-mortality-in-the-usa/#::text=Infant%20mortality%20in%20the%20USA%202021&text=The%20infant%20mortality%20rate%20remained,the%20first%20year%20of%20life, Accessed 03/06/2023.
[35] USA birth certificate, how many people are Born a day in the U.S.?, 2023, https://www.usbirthcertificates.com/articles/people-born-daily#the-number-of-births-a-day-in-the-united-states, Accessed 03/08/2023.
[36] https://www.childrenscolorado.org/conditions-and-advice/conditions-and-symptoms/conditions/pneumonia/, Accessed 03/07/2023.
[37] https://www.asthmaandlung.org.uk/conditions/pneumonia/child/treatment, Accessed 01/17/2024.
[38] https://ourworldindata.org/pneumonia, Accessed 03/08/2023.
[39] S.M. Blower, H. Dowlatabadi, Sensitivity and uncertainty analysis of complex models of disease transmission: an HIV model, as an example, Int. Stat. Rev./Rev. Int. Stat. (1994) 229–243.
[40] C.E. Madubueze, Z. Chazuka, I.O. Onwubuya, F. Fatmawati, C.W. Chukwu, On the mathematical modeling of schistosomiasis transmission dynamics with heterogeneous intermediate host, Front. Appl. Math. Stat. 8 (2022).
[41] S.Y. Tchoumi, C.W. Chukwu, M.L. Diagne, H. Rwezaura, M.L. Juga, J.M. Tchuench, Optimal control of a two-group malaria transmission model with vaccination, Netw. Model. Anal. Health Inform. Bioinform. 12 (1) (2022) 7.
[42] C.W. Chukwu, M.L. Juga, Z. Chazuka, J. Mushanyu, Mathematical analysis and sensitivity assessment of HIV/AIDS-Listeriosis co-infection dynamics, Int. J. Appl. Comput. Math. 8 (5) (2022) 251.
[43] C.W. Chukwu, J. Mushanyu, M.L. Juga, A mathematical model for co-dynamics of listeriosis and bacterial meningitis diseases, Commun. Math. Biol. Neurosci. 2020 (2020) pp.Article-ID.
[44] B.D. Handari, R.A. Ramadhani, C.W. Chukwu, S.H. Khoshnaw, D. Aldila, An optimal control model to understand the potential impact of the new vaccine and transmission-blocking drugs for malaria: A case study in Papua and West Papua, Indonesia, Vaccines 10 (8) (2022) 1174.
[45] C.W. Chukwu, F. Nyabadza, J.K.K. Asamoah, A mathematical model and optimal control for listeriosis disease from ready-to-eat food products, Int. J. Comput. Sci. Math. 17 (1) (2023) 39–49.
[46] J. Mushanyu, C.W. Chukwu, C.E. Madubueze, Z. Chazuka, C.P. Ogbogbo, A deterministic compartmental model for investigating the impact of escapees on the transmission dynamics of COVID-19, Healthc. Anal. 4 (2023) 100275.